Journal of Electrical Systems and Information Technology 3 (2016) 23–32
www.elsevier.com/locate/jesit

# Detection and assessment of partial shading in photovoltaic arrays

Fawzan Salem [a,*], Mohamed A. Awadallah [b]

[a] *Electronics Research Institute (ERI), Egypt*
[b] *University of Zagazig, Egypt*

Received 16 December 2014; accepted 23 October 2015
Available online 18 March 2016

**Abstract**

The paper presents a methodology for detection and assessment of partial shading conditions in photovoltaic (PV) arrays based on artificial neural networks (ANN) as a preliminary step toward automatic supervision and monitoring. The PV array is modeled under normal and partial shading conditions for performance comparison. ANN is designed, trained, and tested for full identification of the partial shading condition. One ANN detects the presence of partial shading and distinguishes it from the uniform change in environmental conditions. If the first ANN detects partial shading on the PV array, other two ANN agents determine the shading factor and infers the number of shaded modules of the array, consequently. Results show excellent performance of ANN on the detection and assessment of partial shading.


*Keywords:* Photovoltaic arrays; Partial shading; Artificial neural networks

## 1. Introduction

Renewable energy has recently attracted increasing attention of the researchers due to cleanliness, on-site availability, and absence of greenhouse gas emission (Salem and Awadallah, 2014). The power of sun light is converted into DC electricity through photovoltaic (PV) cells which are usually made of semiconductor materials. The PV cells are connected in series to form a module of typically 36, 60, or 72 cells. The modules are then assembled in different series and parallel configurations to form an array at the desired output voltage and current. The output power of a PV array is conditioned via power electronic circuitry before being consumed by local loads or injected into power grids.

The output characteristics of the PV arrays are dependent on solar irradiation and cell temperature as the independent variables of the system. However, solar irradiation on a certain array may not be uniform due to partial shading caused by the shadows of passing clouds, trees, or nearby buildings. Many researchers have studied the characteristics of PV arrays under partial shading condition. A mathematical model is developed in Matlab environment and experimentally

* Corresponding author.
*E-mail addresses:* fawzan@eri.sci.eg (F. Salem), awadalla@ksu.edu (M.A. Awadallah).
Peer review under the responsibility of Electronics Research Institute (ERI).

ELSEVIER Production and hosting by Elsevier

http://dx.doi.org/10.1016/j.jesit.2015.10.003

verified for partially shaded solar panels (Patel and Agarwal, 2008). A Simulink model utilizing SimPowerSystems blockset is also developed to model the PV array under the same condition (Said et al., 2012). Artificial neural networks (ANN) are exploited to estimate the *I–V* characteristics under partial shading conditions (Dolan et al., 2011).

It is found from these publications, and others, that the *P–V* curve under partial shading, unlike normal operation, has multiple peaks, whose number depends on the array topology, making maximum power point tracking (MPPT) more challenging. In Karatepe et al. (2007), a novel power compensation and MPPT control system is presented for PV arrays under complicated non-uniform irradiation conditions. The proposed system is based on forward biasing bypass diode of shaded modules by monitoring dynamic resistance and voltage of PV modules. Another MPPT, taking into account shading effects and utilizing a multi-stage buck-boost chopper circuit, is introduced in (Bellini et al., 2010). It proposes a new MPPT algorithm to maximize the power produced in any given ambient/junction temperature and solar irradiation levels.

Provision of early automatic diagnosis of PV arrays with quick and efficient responses is highly necessary and has been studied by many researchers (Chao et al., 2008; Davarifar et al., 2013; Houssein et al., 2010; Syafaruddin et al., 2011; Rezgui et al., 2014). Since the accuracy, fast computation and simplicity are imperative issues in this kind of study, ANN, as an intelligent technique, can be a prominent solution.

Detection and assessment of partial shading is vital for monitoring and supervising purposes as well as invoking appropriate model predictive control MPPT algorithms. A simplified expression could be used to monitor the equivalent thermal voltage in order to detect partial shades on small areas (Sera et al., 2009). In Spataru et al. (2012), fuzzy inference systems are employed to detect partial shading through the associated increase in series resistance of partially shaded cells. Therefore, it appears that the available literature lacks a straightforward method of partial shading detection and assessment based on direct simple measurement of array performance.

The present paper introduces a methodology based on ANN for the automatic detection and assessment of partial shading conditions in PV arrays. The real-time detection and full assessment of the proposed technique help initiate appropriate MPPT algorithm and avoid local overheating of cells. Moreover, it is considered one of the crucial steps toward automatic supervision and system monitoring.

The research assumes that the PV array is initially operating at maximum power point under normal conditions of uniform solar irradiation and cell temperature at all modules. A change in the output power of the array may be due to a consistent change in irradiation or temperature on the whole array, or may be due to partial shading where some modules receive less irradiation than others. A partial shading detection ANN is developed to distinguish between the two cases. If partial shading is detected, the condition is fully assessed by determining the shading factor and number of shaded modules. Therefore, other two ANN operate to assess the condition in case partial shading is characterized by the detection ANN. The design, training, and testing phases of ANN development are meant to be completed offline; then, it should be implemented on fixed-point microprocessor to perform the detection and assessment tasks online.

## 2. PV modeling and problem formulation

A solar cell can be modeled with a current source in parallel to a diode, a shunt resistor to provide a path for leakage current, and a series resistor to account for power loss associated with cell current, Fig. 1(a). The cell current is expressed as:

$$I_c = I_{ph} - I_{os}\,[e^{\frac{q}{AKT}(V_c+I_cR_s)} - 1] - \frac{(V_c + I_cR_s)}{R_{sh}} \tag{1}$$

where $I_c$ is the cell current (A), $I_{ph}$ is the light-generated current, or photocurrent (A), $I_{os}$ is the reverse saturation current of the diode (A), $q$ is the electron charge (C), $A$ is the ideality factor of the diode, $K$ is the Boltzmann constant (J/K), $T$ is the cell temperature (K), $V_c$ is the cell voltage (V), $R_s$ is the series resistance (Ω), and $R_{sh}$ is the shunt resistance (Ω).

The photocurrent is dependent on the solar irradiation and cell temperature, and is given as:

$$I_{ph} = \lambda\,[I_{sc} + k_i(T - T_r)] \tag{2}$$

where λ is the solar irradiation (as a ratio of 1000 W/m$^2$) (suns), $I_{sc}$ is the cell S.C. current at a 25 °C and 1000 W/m$^2$ (A), $k_i$ is the S.C. current temperature coefficient (A/K), $T$ and $T_r$ are the actual and reference temperature (K).

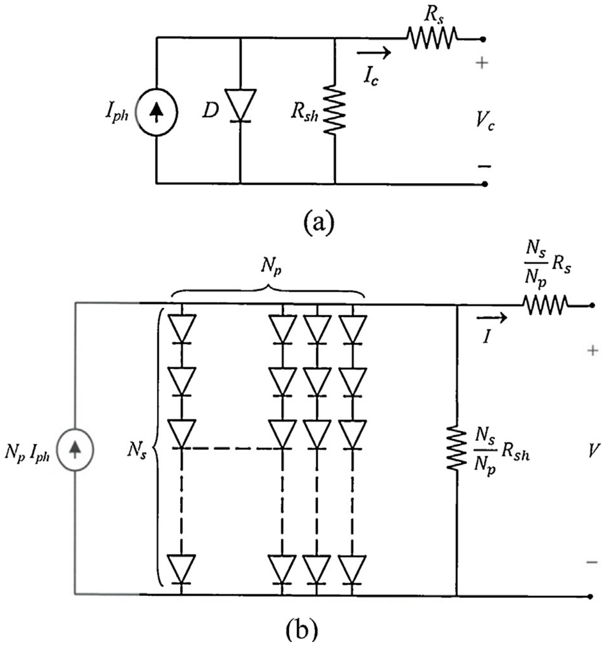


Fig. 1. Equivalent circuits: (a) PV cell, (b) PV array.

On the other hand, reverse saturation current of the diode varies with temperature, and can be expressed as.

$$I_{os} = I_{or}\left(\frac{T}{T_r}\right)^3 e^{\frac{qE_g}{AK}\left(\frac{1}{T_r}-\frac{1}{T}\right)} \tag{3}$$

where $I_{or}$ is the reverse saturation current at reference temperature and irradiation (A), $E_g$ is the band-gap energy of the semiconductor used in the cell (J/C).

The shunt resistance, $R_{sh}$, is inversely related with shunt leakage current to the ground. In general, the PV efficiency is insensitive to variation in such resistance, which can be assumed to approach infinity with no leakage current to ground. Moreover, a small variation in $R_s$ will significantly affect the PV output power. Therefore, the shunt resistance is usually neglected in the cell equivalent circuit.

Since a typical crystalline semiconductor PV cell produces less than 2 W at 0.5 V approximately, the cells must be connected, typically in series, on a module to produce enough high power. A PV array is a group of several modules which are electrically connected in series and parallel to generate the required current and voltage levels. The equivalent circuit of a solar array with $N_s$ and $N_p$ series and parallel cells is shown in Fig. 1(b). The terminal equation of the array current becomes as follows.

$$I = N_p I_{ph} - N_p I_{os}\,[e^{\frac{q}{AKT}\left(\frac{V}{N_s}+\frac{IR_s}{N_p}\right)} - 1] - \frac{1}{R_{sh}}\left[\frac{N_p}{N_s}V + IR_s\right] \tag{4}$$

The above equations are directly employed to obtain the current–voltage characteristics of the PV array. It is evident that the irradiation impact on the output curves is much more significant than that of temperature, especially at the short-circuit point. However, temperature affects open-circuit voltage of the array slightly more notably than irradiation.

Under partial shading operation, the unshaded modules of the PV array receive solar irradiation at certain level, while the shaded modules receive lesser irradiation. The partial shading operating condition is characterized by the shading factor and number of shaded modules. The shading factor is defined in the present paper as the ratio of the irradiation on shaded modules to that on unshaded modules. It is assumed that all modules operate at the same temperature as partial shading is not likely to create substantial temperature difference between shaded and unshaded modules.

Modeling of the solar array under partial shading operation is a two-step process (Patel and Agarwal, 2008). In the first step, two separate I-V curves are produced using Eqs. (1)–(4) for PV modules working under different levels of solar irradiation. The two curves cover the operating regions between the corresponding short-circuit and open-circuit points.

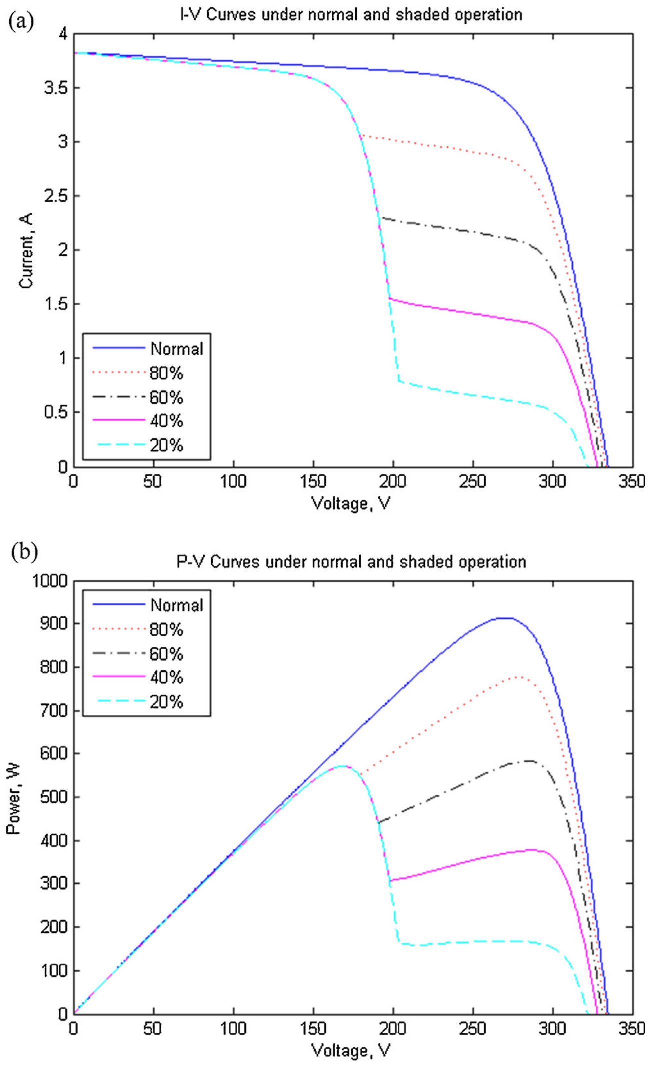


Fig. 2. Output characteristics of the PV array at 800 W/m$^2$ and 300 K under normal operation and 6 shaded modules with different shading factors: (a) *I–V* curves, (b) *P–V* curves.

In the second step, the *I–V* curves are combined together, based on the electrical connection and numbers of shaded and unshaded modules, to produce one curve representing the whole array. Combining curves of series-connected modules implies that, at a certain current value, total voltage is the summation of all module voltages corresponding to the same current as per the individual curves. However, curves of parallel connected modules are combined such that the total current at a given voltage is the summation of individual module currents. The model used in the present paper is experimentally verified in (Patel and Agarwal, 2008).

The impact of shading factor and number of shaded modules on array outputs is depicted in Figs. 2 and 3, respectively. The array characteristics at 800 W/m$^2$ and 300 K are shown in Fig. 2 under normal operation and six shaded modules with different shading factors. The array short-circuit current appears to be unaffected by the shading factor as shown in Fig. 2(a). However, from Fig. 2(b), it is clear that maximum power points are obtained at voltage values which are very close to each other. At the same solar irradiation and cell temperature, Fig. 3 shows the array characteristics with 40% shading factor and different numbers of shaded modules. The number of shaded modules has no effect on the array short-circuit current either, Fig. 3(a); whereas, the voltage at maximum power changes significantly with the number of shaded modules as indicated in Fig. 3(b). It is evident from Figs. 2 and 3 that the present array topology (16 modules connected in series) maintains two local maximum power points under any partial shading condition. It

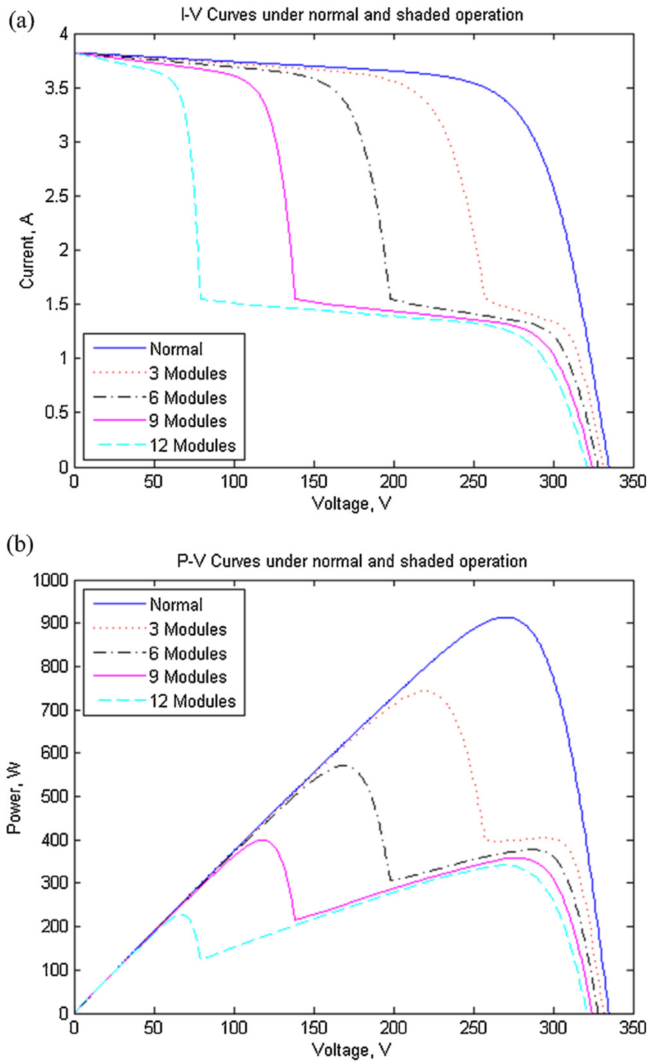


Fig. 3. Output characteristics of the PV array at 800 W/m$^2$ and 300 K under normal operation and 40% shading factor with different shaded modules: (a) *I–V* curves, (b) *P–V* curves.

should be emphasized that the behavior of *I–V* and *P–V* characteristics, as well as the number of local maxima on the power curve, are dependent on the series-parallel configuration of the array.

A change in the array output power could be due to consistent variation of irradiation or temperature affecting all modules, or could be due to partial shading. Since the irradiation change takes place abruptly and unpredictably, the MPPT controller requires some time to respond to the disturbance and track the new maximum power. Before the controller responds, the output voltage of the array remains unchanged as the battery voltage is constant and chopper duty ratio has not been varied yet. Therefore, the momentary change of the array output power occurs at constant voltage, and the operating point moves vertically as shown in Fig. 4.

Assuming a uniform reduction of irradiation on all modules, the new operating condition of the array is normal. Accordingly, the *P–V* curve of the array moves down and the operating point shifts vertically, under constant voltage, from A to B as shown in Fig. 4. Nevertheless, if the reduction of output power is due to partial shading, the operating point moves from A to C instead, Fig. 4. It is among the objectives of the present research to detect whether the new operating condition, upon a change of the array output power, is normal or partial shading. In case partial shading operation is detected, the condition is to be fully assessed by deducing the shading factor and number of shaded modules. Successful detection and precise assessment of partial shading are essential for the MPPT controller to

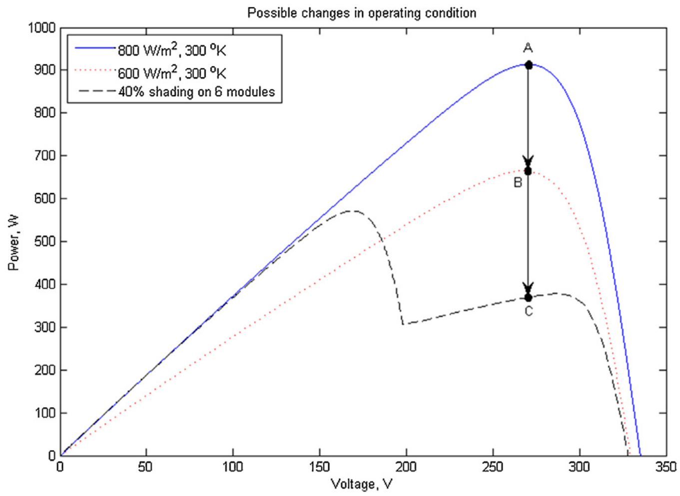


Fig. 4. Instantaneous change in operating condition.

invoke the suitable algorithm and track the maximum power. Moreover, it is considered the first step toward system monitoring and supervision. It should be highlighted that MPPT under partial shading conditions is out of the scope of the present paper. However, detection and assessment of partial shading are accomplished using ANN agents.

## 3. Artificial neural networks (ANN)

One of the earliest artificial intelligence paradigms is ANN (Haykin, 2009; Fausett, 1994), which mimics data processing in a human brain through biological neural networks. The multi-layer feedforward perceptron ANN is composed of processing units called neurons arranged in layer architecture, Fig. 5. An input layer receives the input signals, an output layer yields the outputs, and one or more hidden layers process the signals internally. The operation of artificial neurons is inspired by their natural counterparts. Each neuron has several weighted input signals and one output, where the relationship between the summed inputs and output is governed by a fixed activation function. Weights of the input signals along with the activation function type determine the performance of a neuron, and hence, the whole ANN.

A back-propagation algorithm is employed on the ANN to adapt the weights associated with its links in order to minimize the error between its outputs and a targeted training dataset. Number of neurons in the input and output layers is respectively equal to the number of actual inputs and outputs of the real system represented by the ANN. However, the number of hidden layers and their neurons is chosen by the user via a design process. Researchers have proven that most of nonlinear engineering systems could be represented by a single hidden layer network with varying number of neurons and type of activation function. The computational effort invested on the training process depends mainly on

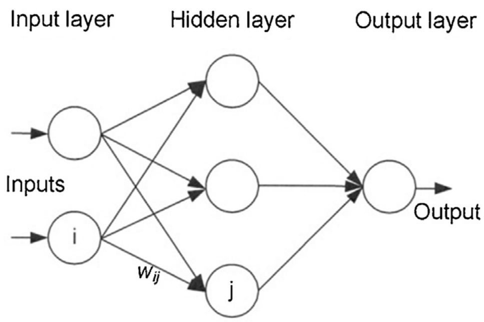


Fig. 5. A two-input one-output multi-layer perceptron feedforward ANN.

the number of modifiable parameters, i.e., weights of the network links. The total number of adaptable weights in a network, with one hidden layer, is given by

$$N_w = N_h(N_i + N_o) \tag{5}$$

where $N_w$ is the total number of weights, $N_h$ is the number of neurons in the hidden layer, $N_i$ is the number of inputs, and $N_o$ is the number of outputs.

The network performance is evaluated through a MSE, Eq. (6), measuring the difference between the actual and targeted ANN outputs of training or testing data. Inspired by natural intelligence, ANN is capable of system modeling, nonlinear mapping, pattern recognition, supervised and unsupervised learning, and problem solving.

$$MSE = \sqrt{\frac{\sum_{i=1}^{N}(T_i - O_i)^2}{N}} \tag{6}$$

where $N$ is the number of data points, $T_i$ is the targeted output at the $i$th data point, $O_i$ is the actual ANN output at the $i$th data point.

## 4. Results and discussion

Detection and assessment of partial shading condition of solar arrays is automated through ANN. Real time measurements of the array are used to detect whether a change in the operating condition is due to partial shading, and then the new condition is assessed in terms of the shading factor and number of shaded modules. Automatic detection and assessment of partial shading help avoid local overheating of cells if blocking and bypass diodes are not present, and help also initiate a suitable MPPT algorithm. The instantaneous shift of PV array operation takes place at constant array voltage accompanied with variations in the characteristic curves of the array. Such variations are employed to detect and assess partial shading using ANN. Most MPPT algorithms implemented in commercially available solar array inverters use frequent measurements of open-circuit voltage and short-circuit current to track maximum power. The existing instruments are used to measure the output voltage and current of the array in order to sense any change in the output power. In case of power change, a detection ANN operates to check for partial shading. If partial shading is detected, two other networks assess the condition by determining the shading factor and number of shaded modules. Outputs of the assessing ANNs are expected to help in the MPPT algorithm under partial shading. As shown in Figs. 2(b) and 3(b), the voltage corresponding to maximum power point depends on the shading factor and number of shaded modules.

### *4.1. Detection of partial shading*

The shift from a normal condition to a partial shading condition is accompanied with a change in the array output power as shown in Fig. 4, almost with no variation in the short circuit current as shown in Figs. 2(a) and 3(a). Such an observation sets forth the basis for the detection of partial shading condition. On the other hand, the uniform change in cell temperature of the PV array results is small variation in the output power and short circuit current.

In reality, the instantaneous sharp change in temperature is nearly impossible as it happens gradually. Nevertheless, cases of small temperature change are taken into account as normal conditions for the sake of generality and robustness of ANN performance. One obvious benefit of including temperature changes as normal conditions in the training data is to make ANN immune against random and systematic measuring errors. The reason is that temperature change yields small variations of output power and short-circuit current. Training ANN on such small variations as normal conditions helps ANN give the right output in case similar size variations are due to measuring errors.

Therefore, the change in output power and short circuit current are used to detect partial shading. The detection ANN takes the relative absolute change in both output power and short circuit current as inputs. The output is zero if the new condition is normal and one if it is partial shading. The relative absolute change in any variable, $x$, depends on the initial and new values, and is given as

$$RAC = \frac{|x_{new} - x_0|}{x_0} \tag{7}$$

Table 1
Testing results of shading detection ANN.

| Case | Initial condition | | New condition | ANN output | |
|---|---|---|---|---|---|
| | $R$ (W/m$^2$) | $T$ (K) | | Ideal | Actual |
| 1 | 928 | 307.2 | $T$ decreases by 1.3 | 0 | –0.0355 |
| 2 | 520 | 291.1 | $R$ increases by 129 | 0 | –0.0065 |
| 3 | 609 | 294.7 | $R$ decreases by 183 | 0 | 0.0027 |
| 4 | 723 | 314.2 | 33% irradiation on 7 modules | 1 | 1.0216 |
| 5 | 988 | 309.4 | 86% irradiation on 1 module | 1 | 1.0394 |
| 6 | 461 | 292.9 | 29% irradiation on 4 modules | 1 | 1.0214 |
| 7 | 384 | 291.8 | 17% irradiation on 2 modules | 1 | 1.0087 |
| 8 | 807 | 299 | 47% irradiation on 7 modules | 1 | 1.0035 |
| 9 | 1066 | 322 | 9% irradiation on 3 modules | 1 | 1.0086 |
| 10 | 317 | 288.4 | 37% irradiation on 8 modules | 1 | 1.0016 |

The training dataset of detection ANN contains 1204 normal operation points resulting from uniform change in solar irradiation or small change in cell temperature on the whole array. Normal operation covers the irradiation range of 300–1000 W/m$^2$, and the temperature range of 290–320 K. Temperature changes are limited to $\pm 1$ or 2 K. The training dataset also contains 6615 partial shading conditions covering the same irradiation and temperature ranges with shading factors from 10% to 90% and shaded modules from 2 to 14.

In the present work, a three-layer ANN, having 20 neurons in the hidden layer, has been used, together with a tansigmoidal activation function and supervised training via a back-propagation technique. The mean square error (MSE) of the training data MSE stagnated at 0.058 after 7 training epochs. It should be mentioned that all networks of the present work are developed using the Neural Networks Toolbox of Matlab 7.8.

Detection ANN is tested using 50 random cases which do not belong to the training dataset. Some of the testing points are slightly outside the training range. Selected testing results of the detection ANN, given in Table 1, show the effectiveness of detection and notable ability to differentiate between normal and partial shading cases.

### 4.2. *Assessment of shading factor*

The comprehensive assessment of a partial shading condition includes the determination of the shading factor and number of shaded modules. The shading factor signifies the ratio of the lesser irradiation on the shaded modules to the higher irradiation on the rest of the array. Once a partial shading condition is detected by the first ANN, two other ANNs are invoked to assess the condition by determining the shading factor and revealing the number of shaded modules.

The shading factor is deduced through a two-input one-output ANN. Inputs are the maximum power at which the system operated before partial shading and the relative absolute change of output power due to shading. ANN output represents the shading factor of the solar array in per unit. Training data contain 12,495 operating point covering the ranges of solar irradiation of 300–1000 W/m$^2$, cell temperature of 290–320 K, shaded modules of 3–15, and shading factor of 10–90%. After 9 training epochs, the MSE reaches a minimum of 0.067. ANN is tested at 50 random points which do not belong to the training data. Some of the testing points are slightly outside the training range. Testing results at 10 selected points are shown in Table 2 indicating high effectiveness in assessing the shading factor. Testing results denote that ANN could recognize, with acceptable accuracy, when some modules (ranging from 2 to 14) receive 90% of the irradiation received by the rest of the PV array. ANN could equally precisely identify cases with light or heavy partial shading on few or many modules as shown by the sample testing results of Table 2.

### 4.3. *Assessment of shaded modules*

Another ANN is developed to deduce the number of shaded modules in case partial shading operation is detected. It is noticed from Figs. 2(b) and 3(b) that the number of shaded modules is identifiable if the shading factor is known in advance. Accordingly, the output of the shading factor assessment ANN is used as an input to the shaded modules assessment ANN. An advantage of ANN is that the number of inputs could be noticeably increased without great increase of the computational burden during the training phase. The inputs are increased to be maximum power before

Table 2
Testing results of shading factor assessment ANN.

| Case | Initial condition | | Partial shading condition | | ANN output | |
|---|---|---|---|---|---|---|
| | $R$ (W/m$^2$) | $T$ (K) | Shading factor | Modules | Ideal | Actual |
| 1 | 823 | 295 | 40% | 12 | 0.4 | 0.3893 |
| 2 | 645 | 315 | 80% | 7 | 0.8 | 0.8255 |
| 3 | 874 | 304 | 90% | 5 | 0.9 | 0.9121 |
| 4 | 927 | 304 | 40% | 14 | 0.4 | 0.4112 |
| 5 | 566 | 296 | 90% | 4 | 0.9 | 0.9081 |
| 6 | 337 | 311 | 60% | 9 | 0.6 | 0.6123 |
| 7 | 566 | 296 | 90% | 4 | 0.4 | 0.4212 |
| 8 | 484 | 296 | 20% | 8 | 0.2 | 0.2123 |
| 9 | 858 | 308 | 80% | 12 | 0.8 | 0.8288 |
| 10 | 643 | 308 | 90% | 10 | 0.9 | 0.8788 |

Table 3
Testing results of shaded modules assessment ANN.

| Case | Initial condition | | Partial shading condition | | ANN output | |
|---|---|---|---|---|---|---|
| | $R$ (W/m$^2$) | $T$ (K) | Shading factor | Modules | Ideal | Actual (rounded) |
| 1 | 694 | 294 | 13.3% | 5 | 5 | 5 |
| 2 | 744 | 298 | 14.6% | 3 | 3 | 3 |
| 3 | 737 | 294 | 29.9% | 9 | 9 | 9 |
| 4 | 908 | 303 | 52.4% | 11 | 11 | 11 |
| 5 | 815 | 302 | 53.3% | 5 | 5 | 5 |
| 6 | 848 | 300 | 62.4% | 11 | 11 | 11 |
| 7 | 496 | 312 | 71.2% | 3 | 3 | 3 |
| 8 | 547 | 312 | 78% | 2 | 2 | 2 |
| 9 | 404 | 303 | 84.8% | 3 | 3 | 3 |
| 10 | 614 | 302 | 12.9% | 6 | 6 | 6 |

partial shading, relative absolute change in power due to shading, and shading factor as inferred by shading factor assessment ANN.

The training dataset are divided into three groups including 28,512 points and covering the operating range of 400–950 W/m$^2$ irradiation, 293–313 K cell temperature, 0.1–0.9 shading factor, and 1–12 shaded modules. The training MSE stagnates, in average, at 0.788 after 26 epochs. The ANN agents are tested at random points, within the training range, which do not belong to the training data. The matching between the actual number of shaded modules and ANN output, rounded to the nearest integer, is excellent. A sample of 10 testing points, shown in Table 3, indicates remarkable effectiveness in assessing shaded modules under partial shading operation.

The methodology of ANN development, presented in this paper, could be extended to other operating ranges or array topologies. Other series-parallel configurations of solar arrays provide different output characteristic curves and different numbers of local power maxima. Consequently, ANN agents should be entirely developed from the beginning for other array topologies.

## 5. Conclusion

The paper presents a methodology based on ANN for the detection and assessment of partial shading conditions in solar PV arrays. The array consists of 16 series modules each has 36 PV cells connected in series. The PV array is simulated under normal and partial shading conditions using a Matlab model which was experimentally validated in the literature. When a change in the PV array output power takes place, a detection ANN is able to distinguish whether the new operating condition is partial shading or not.

In case partial shading is detected, two other ANNs are able to fully assess the shading factor and number of shaded modules of the PV array. ANN testing show distinct effectiveness with acceptable accuracy in the detection and assessment of partial shading conditions of solar PV arrays. The proposed technique could be straightforwardly extended to cover different operating ranges of the given PV array, or to consider other array topologies as well.

## Appendix I. Simulation parameters

| PV array | |
|---|---|
| Number of modules per array | 16 |
| Number of cells in series | 36 |
| Reference reverse saturation current | $2.35 \times 10^{-8}$ A |
| Short-circuit current temperature coefficient | 0.0021 A/K |
| Diode ideality factor | 1.21 |
| Series resistance per cell | 0.01143 Ω |
| Shunt resistance per cell | 4.16667 Ω |

## References

Bellini, A., Bifaretti, S., Iacovone, V., 2010. MPPT algorithm for current balancing of partially shaded photovoltaic modules. In: IEEE International Symposium on Industrial Electronics (ISIE), pp. 933–938.

Chao, K.H., Ho, S.H., Wang, M.H., 2008. Modeling and fault diagnosis of a photovoltaic system. Electric Power Systems Res 78 (1), 97–105.

Davarifar, M., Rabhi, A., El-Hajjaji, A., Dahmane, M., 2013. Real-time model base fault diagnosis of PV panels using statistical signal processing. In: Proceedings of the Intrenational Conference on Renewable Energy Research and Applications, Spain, pp. 599–604, Oct. 20-23.

Dolan, J.A., Lee, R., Yeh, Y., Daniel, C., Nguyen, Y., Ben-Menahem, S., Ishihara, A., 2011. Neural network estimation of photovoltaic *I–V* curves under partially shaded conditions. In: Proceeding of International Joint Conference in Neural Networks, San Jose, CA, USA, pp. 1358–1365.

Fausett, L.V., 1994. Fundamentals of Neural Networks: Architectures, Algorithms, and Applications. Prentice Hall International.

Haykin, S., 2009. Neural Networks and Learning Machines, 3rd edition. Prentice Hall.

Houssein, A., Heraud, N., Souleiman, I., Pellet, G., 2010. Monitoring and fault diagnosis of photovoltaic panels. In: Proceedings of the IEEE International Energy Conference and Exhibition, Manama, Bahrain, December 18–22, pp. 389–394.

Karatepe, E., Kumamoto, Hiyama, T., Boztepe, M., Colak, M., 2007. Power controller design for photovoltaic generation system under partially shaded insolation conditions. In: ISAP 2007, International Conference on Intelligent Systems Applications to Power Systems, pp. 1–6.

Patel, H., Agarwal, V., 2008. MATLAB-based modeling to study the effects of partial shading on PV array characteristics. IEEE Trans. Energy Convers. 23 (1), 302–310, March.

Rezgui, W., Mouss, H., Mouss, M.D., Kadri, O., 2014. Electrical faults detection for the intelligent diagnosis of a photovoltaic generator. J. Electrical Eng. 14 (1), 77–84.

Said, S., Massoud, A., Benammar, M., Ahmed, S., 2012. A Matlab/Simulink-based photovoltaic array model employing SimPowerSystems toolbox. J. Energy Power Eng. 6, 1965–1975.

Salem, F., Awadallah, M.A., 2014. Parameters estimation of photovoltaic modules: comparison of ANN and ANFIS. Int. J. Indus. Electron Drives 1 (2), 121–129.

Sera, D., Teodorescu, R., Rodriguez, P., 2009. Partial shadowing detection based on equivalent thermal monitoring for PV module diagnostics. In: Proceedings of the Annual Conference of the IEEE Industrial Electronics Society, Porto, Portugal, November 3–5, pp. 708–713.

Spataru, S., Sera, D., Kerekes, T., Teodorescu, R., 2012. Detection of increased series losses in PV arrays using fuzzy inference systems. In: Proceedings of the IEEE Photovoltaic Specialists Conference, Austin, TX, USA, June 3–8, pp. 464–469.

Syafaruddin, E., Karatepe, T., Hiyama, 2011. Controlling of artificial neural network for fault diagnosis of photovoltaic array. In: Proceedings of the International Conference on Intelligent System Application to Power Systems, Hersonissos, Greece, September 25–28, pp. 1–6.